JCI The Journal of Clinical Investigation

Metabolic acidosis stimulates H+ secretion in the rabbit outer medullary collecting duct (inner stripe) of the kidney.

S Tsuruoka, G J Schwartz

J Clin Invest. 1997;99(6):1420-1431. https://doi.org/10.1172/JCI119301.

Research Article

The outer medullary collecting duct (OMCD) absorbs HCO3- at high rates, but it is not clear if it responds to metabolic acidosis to increase H+ secretion. We measured net HCO3- transport in isolated perfused OMCDs taken from deep in the inner stripes of kidneys from control and acidotic (NH4Cl-fed for 3 d) rabbits. We used specific inhibitors to characterize the mechanisms of HCO3- transport: 10 microM Sch 28080 or luminal K+ removal to inhibit P-type H+,K+-ATPase activity, and 5-10 nM bafilomycin A1 or 1-10 nM concanamycin A to inhibit H+-ATPase activity. The results were comparable using either of each pair of inhibitors, and allowed us to show in control rabbits that 65% of net HCO3- absorption depended on H+-ATPase (H flux), and 35% depended on H+,K+-ATPase (H,K flux). Tubules from acidotic rabbits showed higher rates of HCO3- absorption (16.8+/-0.3 vs. 12.8+/-0.2 pmol/min per mm, P < 0.01). There was no difference in the H,K flux (5.9+/-0.2 vs. 5.8+/-0.2 pmol/min per mm), whereas there was a 61% higher H flux in segments from acidotic rabbits (11.3+/-0.2 vs. 7.0+/-0.2 pmol/min per mm, P < 0.01). Transport was then measured in other OMCDs before and after incubation for 1 h at pH 6.8, followed by 2 h at pH 7.4 (in vitro metabolic acidosis). Acid incubation in vitro stimulated HCO3- absorption (12.3+/-0.3 to […]

Metabolic Acidosis Stimulates H^+ Secretion in the Rabbit Outer Medullary Collecting Duct (Inner Stripe) of the Kidney

Shuichi Tsuruoka and George J. Schwartz
Department of Pediatrics and Department of Medicine, University of Rochester School of Medicine, Rochester, New York 14642

Abstract

The outer medullary collecting duct (OMCD) absorbs HCO_3^- at high rates, but it is not clear if it responds to metabolic acidosis to increase H^+ secretion. We measured net HCO_3^- transport in isolated perfused OMCDs taken from deep in the inner stripes of kidneys from control and acidotic (NH_4Cl-fed for 3 d) rabbits. We used specific inhibitors to characterize the mechanisms of HCO_3^- transport: 10 μM Sch 28080 or luminal K^+ removal to inhibit P-type H^+,K^+-ATPase activity, and 5–10 nM bafilomycin A_1 or 1–10 nM concanamycin A to inhibit H^+-ATPase activity. The results were comparable using either of each pair of inhibitors, and allowed us to show in control rabbits that 65% of net HCO_3^- absorption depended on H^+-ATPase (H flux), and 35% depended on H^+,K^+-ATPase (H,K flux). Tubules from acidotic rabbits showed higher rates of HCO_3^- absorption (16.8±0.3 vs. 12.8±0.2 pmol/min per mm, $P < 0.01$). There was no difference in the H,K flux (5.9±0.2 vs. 5.8±0.2 pmol/min per mm), whereas there was a 61% higher H flux in segments from acidotic rabbits (11.3±0.2 vs. 7.0±0.2 pmol/min per mm, $P < 0.01$). Transport was then measured in other OMCDs before and after incubation for 1 h at pH 6.8, followed by 2 h at pH 7.4 (in vitro metabolic acidosis). Acid incubation in vitro stimulated HCO_3^- absorption (12.3±0.3 to 16.2±0.3 pmol/min per mm, $P < 0.01$), while incubation at pH 7.4 for 3 h did not change basal rate (11.8±0.4 to 11.7±0.4 pmol/min per mm). After acid incubation the H,K flux did not change, (4.7±0.4 to 4.6±0.4 pmol/min per mm), however, there was a 60% increase in H flux (6.6±0.3 to 10.8±0.3 pmol/min per mm, $P < 0.01$). In OMCDs from acidotic animals, and in OMCDs incubated in acid in vitro, there was a higher basal rate and a further increase in HCO_3^- absorption (16.7±0.4 to 21.3±0.3 pmol/min per mm, $P < 0.01$) because of increased H flux (11.5±0.3 to 15.7±0.2 pmol/min per mm, $P < 0.01$) without any change in H,K flux (5.4±0.3 to 5.6±0.3 pmol/min per mm).

These data indicate that HCO_3^- absorption (H^+ secretion) in OMCD is stimulated by metabolic acidosis in vivo and in vitro by an increase in H^+-ATPase-sensitive HCO_3^- absorption. The mechanism of adaptation may involve increased synthesis and exocytosis to the apical membrane of proton pumps. This adaptation helps maintain homeostasis during metabolic acidosis. (*J. Clin. Invest.* 1997. 99:1420–1431.) Key words: H^+-ATPase • bicarbonate absorption • H^+,K^+-ATPase • regulation • acidification

Introduction

The kidney responds to the pathophysiologic entity of metabolic acidosis by increasing urinary acidification to restore homeostasis. Adaptation to acidosis occurs at the level of the proximal tubule, whereby increased brush border Na^+/H^+ antiporter activity and increased basolateral $Na^+(HCO_3^-)_3^{2-}$ cotransport occur (1, 2). In the distal nephron the cortical collecting duct (CCD)[1] reverses the polarity of its flux from secreting HCO_3^- to secreting protons (3), and the inner medullary collecting duct (IMCD) increases H^+ secretion rate (4–6).

Under baseline conditions, the outer medullary collecting duct (OMCD) has the highest rate of H^+ secretion (HCO_3^- absorption) of the collecting duct segments (7). If this segment were capable of enhancing its rate of transport during metabolic acidosis, it could contribute greatly to the restoration of acid–base homeostasis. Whether or not the outer medullary collecting duct (OMCD) adapts to metabolic acidosis remains unclear. Most investigators (8–11) have detected no change in HCO_3^- transport or steady state luminal pH (12) after in vivo metabolic acidosis. Indeed, in a major review of intercalated cell function, Schuster noted that "surprisingly, none of the studies of chronic acidosis using oral acid loading or chronic high P_{CO_2} exposure has resulted in a significant alteration in the rate of net HCO_3^- reabsorption (H^+ secretion) by rat or rabbit OMCD."

An exception was reported by McKinney and Davidson (13), who found HCO_3^- absorption rate to be increased after acutely raising P_{CO_2}. Moreover, there is definite morphological evidence for adaptation of the OMCD to chronic acidosis as seen by the increased apical surface density and decreased apical cytoplasmic tubulovesicular structures (14, 15), as well as by increased apical labeling of H^+-ATPase, increased basolateral membrane labeling of band 3, and decreased band 3 labeling of multivesicular bodies of intercalated cells (15).

The pathways for HCO_3^- absorption in the OMCD have been recently identified. The rabbit OMCD absorbs HCO_3^-, believed in large part to occur via an apical H^+-ATPase in series with a basolateral Cl^-–HCO_3^- exchanger (16–18). This segment does not actively transport Na^+, K^+, or Cl^- (19), suggesting an absence of typically functioning principal cells. With

Address correspondence to George J. Schwartz, M.D., Professor of Pediatrics and Medicine, Chief, Pediatric Nephrology, Box 777 University of Rochester Medical Center, 601 Elmwood Avenue, Rochester, NY 14642. Phone: 716-275-9784; FAX: 716-273-1038; E-mail: GESC@bphvax.biophysics.rochester.edu

Received for publication 8 July 1996 and accepted in revised form 8 January 1997.

J. Clin. Invest.

0021-9738/97/03/1420/12 $2.00
Volume 99, Number 6, March 1997, 1420–1431

1. *Abbreviations used in this paper:* CCD, cortical collecting duct; IMCD, inner medullary collecting duct; OMCD, outer medullary collecting duct.

regard to the transporters and enzymes required for H^+ secretion, the cells along the inner half of the inner stripe appear qualitatively similar but with different states of functional activity, at least in the rabbit (20–22). Gluck and co-workers have demonstrated that a vacuolar H^+-ATPase is present in the apical membrane of OMCD cells (16, 17, 23). During chronic metabolic acidosis, however, an increase in H^+-ATPase protein and mRNA was not detected (24). Rather, in response to acidosis there was a polarization of H^+ pumps from the cytoplasm to the apical membrane (24). Presumably, this process of apical polarization allows more H^+ pumps to be in contact with the luminal fluid, and hence allows more acidification to occur.

Recent data suggest that, in addition to the vacuolar H^+-ATPase, there might also be an apically oriented P-type gastric-like H^+,K^+-ATPase that mediates HCO_3^- absorption in the OMCD (25–27). Indeed, from a series of inhibitor studies, Armitage and Wingo concluded that the H^+,K^+-ATPase contributes more than does the vacuolar H^+-ATPase to renal acidification in the OMCD (27). The combination of H^+-ATPase and H^+,K^+-ATPase inhibitors totally eliminated net HCO_3^- absorption, indicating that these are the two most important H^+-translocating systems in the OMCD (27).

Given that the transporters mediating the high rate of H^+ secretion in the OMCD have been elicited, it seemed appropriate to investigate if and how these transporters respond to the pathophysiologic stress of metabolic acidosis. The purpose of these studies was to establish the contributions of the vacuolar H^+-ATPase and P-type H^+,K^+-ATPase under control and acidotic conditions. We also investigated whether or not a similar regulation occurs in response to an in vitro model of metabolic acidosis.

Methods

Animals. Female New Zealand white rabbits ($n = 25$) weighing 1.7–3.6 kg and maintained on normal laboratory chow (Purina lab diet 5326; Purina Mills, Richmond, IN) plus free access to tap water were used as control rabbits (Ctl) in this study. The diet provided 0.25% Na, 1.2% K, 0.5% Cl, and 1.1% Ca. An additional group of 23 rabbits of comparable weight (1.8–2.8 kg) was acid-treated (Acid) for 3 d by providing 75 mM NH_4Cl added to a 5% sucrose drinking solution, which yielded an acid equivalent load of 10–15 meq/kg per d, and by limiting food intake to 2% of body weight (28). This treatment has previously been shown to induce reliably metabolic acidosis in rabbits (28, 29).

The animals were weighed and then killed by intracardiac injection of 130 mg pentobarbital sodium after premedication with ketamine (44 mg/kg) and xylazine (5 mg/kg).

Tubule isolation. Kidneys were removed, and 1–2 mm coronal slices were made and transferred to chilled dissection medium containing (mM): 145 NaCl, 2.5 K_2HPO_4, 2 $CaCl_2$, 1.2 $MgSO_4$, 5.5 D-glucose, 1 Na_3 citrate, 4 Na lactate, and 6 L-alanine, pH 7.4, 290±2 mosmol/kg. OMCDs were dissected from the cortico-medullary rays. Attention was made to obtain the ducts from deep within the inner stripe (below the termination of S3 segments and adjacent to the medullary thick ascending limbs of Henle's loop); segments from the outer stripe were deliberately avoided. To maximize the reproducibility of this isolation, relatively short segments (0.5–0.7 mm) were obtained.

In vitro microperfusion. In vitro microperfusion was performed as described by Burg (30) (with modifications) (31–33). An isolated OMCD was rapidly transferred to a 1.2-ml temperature- and environmentally controlled chamber mounted on an inverted microscope, and perfused and bathed with Burg's solution (see Table I) at 37°C under an atmosphere of 94% O_2/6% CO_2 (31–34). The collecting end of the segment was sealed into a holding pipette using Sylgard 184 (Dow Corning Corp., Midland, MI). 14-nl samples of tubular fluid were collected under water-saturated mineral oil by timed filling of a calibrated volumetric pipette. Collections were made in triplicate.

The specimen chamber and perfusate reservoir were continuously suffused with 94% O_2/6% CO_2 to maintain ambient pH at 7.4 (34). The flow rate of bathing solution entering the specimen chamber was maintained at 14 ml/h by a peristaltic pump.

Bicarbonate transport. The concentrations of total CO_2 (assumed to be equal to that of HCO_3^-) in perfusate (C_O) and collected fluid (C_L) were measured by microcalorimetry (Picapnotherm; Microanalytical Instrumentation, Mountain View, CA). Because there is no net water absorption in the OMCD (8, 27, 35), the rate of HCO_3^- transport ($JHCO_3$) was calculated as: $JHCO_3 = (C_O\text{-}C_L)(V_L/L)$, where V_L was the rate of collection of tubular fluid, L the tubular length (in mm), and J was in pmol/min per mm tubular length. We tried to improve the performance of the picapnotherm to prevent any fluid loss by using large flat LiOH granules, replacing them weekly, making volumetric pipettes with long constrictions to assure reproducibility, and by aspirating small amounts of water-saturated mineral oil into the pipette tip after obtaining the sample. When $JHCO_3 > 0$, there was net HCO_3^- absorption equivalent to H^+ secretion. The coefficient of variation for a 20-mM standard measured in quadruplicate by microcalorimetry was $< 0.5\%$ (< 23 counts per sample of 4,500 counts). This level of sensitivity allowed us to detect reliably HCO_3^- concentration differences of 1 mM between perfused and collected fluids. In practice, we perfused tubules at 3–4 nl/min per mm (1.5–2 nl/min), which generally resulted in a difference of ~ 5 mM between perfused and collected fluids.

Transepithelial voltage (Vte). Transepithelial voltage was measured using the perfusion pipette as an electrode. The voltage difference between calomel cells connected via 3 M KCl agar bridges to perfusing and bathing solutions was measured with a high impedance electrometer (World Precision Instruments, New Haven, CT).

Collections of tubular fluid were initiated once the Vte had stabilized ($\geq$ 45 min), and readings were recorded at the conclusion of each collection and averaged for each protocol.

Viability. Evidence for damaged cells and gross leak of perfusate was continually assessed by the inclusion of 0.15 mg/ml FD & C green dye to all perfusates during the study (31). The experiment was discontinued if there was cellular uptake of the dye.

Experimental protocols. In most protocols, $JHCO_3$ was measured under baseline conditions (with Burg's solution in lumen and bath), and again after H^+ secretion inhibition. Collections were started not less than 45 min after the tubule was brought to 37°C. The vacuolar H^+-ATPase was inhibited using the nM concentrations of the specific inhibitors bafilomycin A_1 and concanamycin A (27, 31, 36, 37). The bafilomycins are macrolide antibiotics with a 16-membered lactone ring originally isolated from *Streptomyces griseus* (38); the concanamycins possess an 18-membered lactone ring, and were first isolated from *Streptomyces diastatochromogenes* (39). In fact, the concanamycins show more than 20 times greater inhibitory effect than the bafilomycins on the vacuolar type ATPase (36), and would therefore be considered superior H^+-ATPase inhibitors. Therefore, a concentration of 1 nM concanamycin A would be expected to inhibit more H^+-ATPase–dependent H^+ secretion than 5 or 10 nM bafilomycin A_1 (36). The P-type H^+,K^+-ATPase was inhibited using 10 μM 2-methyl-8-(phenylmethoxy)imidazol[1,2-α]pyridine-3-acetonitrile (Sch 28080; kindly provided by Dr. T. Sybertz, Schering-Plough Research Institute, Kenilworth, NJ) (25, 31, 40), or removal of luminal potassium (K^+-free, Table I) (27). In an additional protocol, we used Na^+- and K^+-free solutions (Table I), the rationale being to inhibit a colonic-type H^+,K^+-ATPase, or a more promiscuous pump that can transport potassium or sodium in exchange for protons (41). In general, the OMCDs were exposed to inhibitors for 10–15 min before collections were initiated.

3 h incubation. To study adaptation after equilibration and initial collections, we incubated OMCDs for 3 h in vitro. Previously, we had shown that incubation of CCDs for 1 h at pH 6.8 followed by 2 h at pH 7.4 caused a reversal of net HCO_3^- flux from secretion to absorption (31). Because α-intercalated cells showed upregulation of H^+ secretion, we used a similar approach to investigate adaptation of the OMCD of the inner stripe, which is comprised primarily of H^+-secreting cells (20–22). The rationale for dividing the 3-h incubation into a 1-h exposure to low pH followed by a 2-h recovery was based on the expectation that renal cell physiology, metabolism, and protein synthesis would be better maintained at normal ambient pH, and that the adaptive process to respond to the acid stimulus would be facilitated at a higher pH (31).

The control incubation solution was prepared by mixing 3 parts Dulbecco's modified Eagle's medium (DMEM) containing 44 mM $NaHCO_3$ (GIBCO BRL, Gaithersburg, MD), plus 5 parts Burg's solution containing 25 mM $NaHCO_3$ and 1 part HCO_3^--free dissection solution, yielding a HCO_3^- concentration of 28 mM. The acid solution contained 3 parts DMEM without $NaHCO_3$ (GIBCO BRL), plus 2 parts Burg's solution and 4 parts dissection solution, yielding a HCO_3^- concentration of 6 mM (31, 32). Solutions were applied to both apical and basolateral surfaces of the OMCD. The bathing solutions contained 30 U/ml penicillin, 30 μg/ml streptomycin (GIBCO BRL), and 3.3% fetal bovine serum (GIBCO BRL). When the control solution was gassed at 37°C with 6% CO_2, the pH was 7.40±0.02, whereas the acid solution gave a pH of 6.80±0.02.

After the 3-h incubation, collections were generally completed within 2–3 h so that the total time of each experiment was usually 7–8 h.

Chemicals. Bafilomycin A_1 was purchased from Sigma Chemical Co. (St. Louis, MO), and concanamycin A was purchased from Fluka Biochemical Co. (Ronkonkoma, NY). These inhibitors were dissolved in DMSO at 0.1% final concentration. All chemicals were of the highest reagent grade.

Statistics. Results are presented as mean±SE, where n is the number of tubules. Data from each tubule before incubation or inhibition were compared with those from after incubation or inhibition in a paired t test. Comparisons of tubules from normal and acid-treated rabbits were performed by unpaired t test. $P < 0.05$ was considered significant. Statistical comparisons were performed using Number Cruncher Statistical Software (NCSS, Kaysville, UT).

Table I. Composition of Solutions

Solute	Burg's solution	K^+-free	Na^+,K^+-free
	mM	*mM*	*mM*
NaCl	115	115	
K_2HPO_4	2.5		
$CaCl_2$	2.0	2.0	2.0
$MgSO_4$	1.2	1.2	1.2
Na lactate	4.0	4.0	
Na_3 citrate	1.0	1.0	
L-alanine	6.0	6.0	6.0
D-glucose	5.5	5.5	5.5
$NaHCO_3$	25	25	
Na_2HPO_4		2.5	
Choline HCO_3			25
Choline Cl			115
Tris			10

The pH of Tris was 7.4, prepared by mixing Tris-HCl and Tris base. Each solution was gassed with 95% O_2/5% CO_2 at room temperature to attain a pH of 7.4. The osmolality of each solution was 290±2 mosmol/kg. Solutions were assured to be Na^+-or K^+-free by flame photometry.

Results

Dependence of net HCO_3^- absorption on body weight. We determined whether some of the variability in HCO_3^- transport rate could be explained by differences in the size of the rabbits from which they were obtained. In 25 OMCDs taken from control rabbits and perfused and bathed in Burg's solution (Table I) the net HCO_3^- absorptive flux (Fig. 1) averaged 12.8±0.3 pmol/min per mm, while transepithelial voltage averaged 3.6±0.2 mV. There was a highly significant correlation (r = 0.83) between net HCO_3^- flux and body weight of the rabbit from which the segment was obtained. Therefore, to determine the effects of in vivo acidosis on HCO_3^- transport, we studied segments taken from comparably sized control and acidotic animals.

Effect of in vivo acidosis on acid–base status and net HCO_3^- absorption. Blood taken from the hearts of 20 control animals at the time of death yielded a pH of 7.35±0.02, and a [HCO_3^-] of 25.4±0.8 mM, while that from 19 acid-treated animals was significantly lower (pH of 7.18±0.02 and [HCO_3^-] of 16.5±0.8 mM, respectively, $P < 0.01$ for each comparison). Urine taken by postmortem bladder aspiration yielded a pH of 8.0±0.1 in controls vs. 5.1±0.1 in acid-treated animals ($P < 0.01$). When killed, the mean weight of the control rabbits was 2.5±0.1 kg, while that of the acid-treated rabbits was 2.3±0.1 kg (not significantly different).

In 23 OMCDs taken from acid-treated rabbits (Fig. 2) (compared to segments from controls) both net HCO_3^- flux and transepithelial voltage, respectively, were significantly higher (acid, 16.8±0.2 pmol/min per mm and 4.9±0.2 mV vs. control, 12.8±0.3 pmol/min per mm and 3.6±0.2 mV; $P < 0.01$ for both). The flux was 4 pmol (31%) higher, and the voltage was 1.3 mV (36%) higher in segments from acid-treated animals. There was no significant correlation between net HCO_3^- flux and body weight (r = 0.33, data not shown).

Dependence of HCO_3^- absorption on H^+-ATPase and H^+,K^+-ATPase. We used specific inhibitors of the vacuolar H^+-ATPase (5 nM bafilomycin) and of the P-type H^+,K^+-ATPase (10 μM Sch 28080) to determine their effects on net HCO_3^- absorption in isolated perfused OMCDs from the inner stripe. In three segments with a baseline flux of 12.5±0.2 pmol/min per mm, Sch 28080 inhibited the flux by 5.2 pmol (42%) to 7.2±0.5 (Fig. 3, Table II, $P < 0.01$), along with a 0.3 mV de-

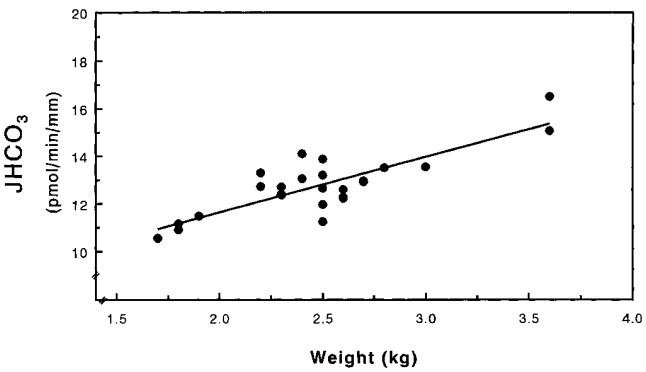

Figure 1. Linear regression of net HCO_3^- transport (J_{HCO_3}) versus body weight. Transport was significantly correlated (r = 0.83, $P <$ 0.01) with body weight of control animals. The equation of the regression line is $y = 7.0 + 2.3x$, n = 25.

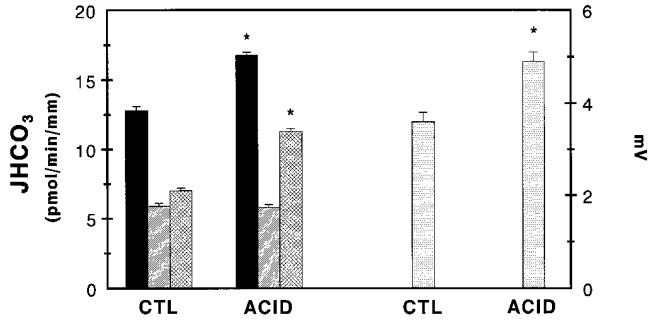

Figure 2. Bicarbonate transport (J_{HCO_3}) data and transepithelial voltage measurements in OMCDs taken from control (*CTL*) and acid-treated (*ACID*) rabbits. *Solid bars*, total net HCO_3^- flux; *slashed bars*, H,K flux; *cross hatched bars*, H flux; *stippled bars*, transepithelial voltage. *Significantly different from respective measurement in CTL tubules ($P < 0.05$).

crease in transepithelial voltage (2.7±0.1 to 2.4±0.1 mV, $P <$ 0.05). Compared to the basal period, the collected fluid HCO_3^- concentration was 1.8 mM higher ($P < 0.05$) after Sch 28080 despite a significantly higher perfusion flow rate (Table II). The subsequent addition of bafilomycin reduced the flux by 6.1 to 1.1±0.3 pmol ($P < 0.01$), and transepithelial voltage decreased by 1.1 to 1.3±0.3 mV ($P < 0.01$). With the addition of bafilomycin, there was a further 2.0-mM increase in collected fluid HCO_3^- concentration ($P < 0.05$) to nearly the perfused concentration.

Similar results were obtained in four segments from acidotic animals with a higher basal flux of 17.1±0.5 pmol/min per mm. Sch 28080 decreased the flux by 5.5 pmol (32%) to 11.6±0.2 pmol (Fig. 3, Table II, $P < 0.01$) as shown for control tubules, but without any statistical change in transepithelial voltage (4.2±0.3 to 4.0±0.5 mV). The collected fluid HCO_3^- concentration increased by 1.9 mM ($P < 0.05$) despite comparable flow rates (Table II). The subsequent addition of bafilomycin reduced the flux by 10.4 pmol (70% greater decrement than in control segments) to 1.2±0.2 pmol ($P < 0.01$), and transepithelial voltage decreased by 1.2 to 1.8±0.3 mV ($P <$ 0.01). Collected fluid HCO_3^- concentration was increased 3.7 mM by bafilomycin ($P < 0.05$), reaching within 0.5 mM of the perfused concentration.

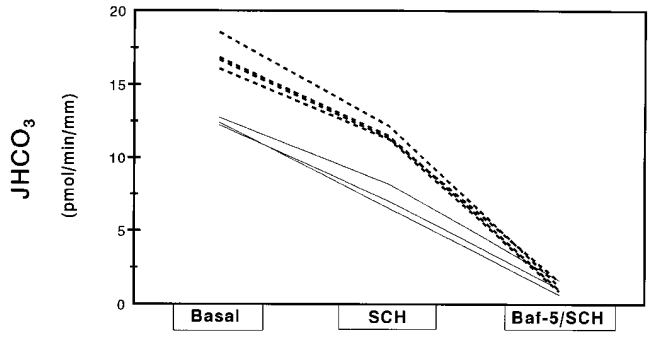

Figure 3. Effect of 10 μM Sch 28080 (*SCH*) plus 5 nM bafilomycin A1 (*Baf-5/SCH*) on net (*Basal*) HCO_3^- flux in OMCDs from control (*solid lines*, $n = 3$) and acid-treated (*dashed wide lines*, $n = 4$) rabbits. Each line represents an individual tubule experiment.

Table II. Mean Transport Data: Effect of Sch 28080 and Bafilomycin

Parameter	Basal	Sch 28080	Sch + Baf 5
Control OMCDs ($n = 3$)			
Tubule length (mm)	0.6±0.1		
Flow rate (nl/min)	1.8±0.1	1.9±0.1*	1.6±0.1
Perf. HCO_3^- (mmol/liter)	24.4±0.1	24.4±0.1	24.4±0.1
Coll. HCO_3^- (mmol/liter)	20.2±0.1	22.0±0.1*	24.0±0.1*‡
J_{HCO_3} (pmol/min per mm)	12.5±0.2	7.2±0.5*	1.1±0.3*‡
Acid OMCDs ($n = 4$)			
Tubule length (mm)	0.7±0.1		
Flow rate (nl/min)	1.9±0.1	1.8±0.1	1.6±0.1
Perf. HCO_3^- (mmol/liter)	24.4±0.1	24.4±0.1	24.3±0.1
Coll. HCO_3^- (mmol/liter)	18.2±0.3	20.1±0.3*	23.8±0.2*‡
J_{HCO_3} (pmol/min per mm)	17.1±0.5	11.6±0.2*	1.2±0.2*‡

OMCDs taken from control (*Control*) and acidotic (*Acid*) animals. Data are mean±SE (SE < 0.05 are rounded to 0.1). Perf. HCO_3^-, perfusion concentration of HCO_3^-; Coll. HCO_3^-, collected fluid concentration of HCO_3^-; J_{HCO_3}, net bicarbonate flux. Sch 28080, used at 10 μM; Sch + Baf 5, 10 μM Sch 28080 plus 5 nM bafilomycin. *Significantly different from basal parameter, ‡significantly different from preceding period after basal.

To eliminate any effect of time or agent on the pattern of HCO_3^- transport, we applied bafilomycin before Sch 28080 in seven tubules with a baseline flux of 13.0±0.2 pmol/min per mm (Fig. 4, Table III) and a transepithelial voltage of 3.3±0.3 mV. After adding 5 nM bafilomycin, the flux had decreased by 6.8 pmol (53%) to 6.2±0.3 pmol/min per mm, and voltage had decreased by 1.2 to 2.1±.3 mV ($P < 0.01$ for both changes). Collected fluid HCO_3^- concentration was increased 2.2 mM by bafilomycin ($P < 0.05$) without any change in flow rate (Table III). The subsequent addition of Sch 28080 further decreased net flux by an additional 4.5 pmol to 1.6±0.3 pmol/min per mm ($P < 0.01$) along with a 0.3-mV decrease in transepithelial voltage (to 1.8±0.3 mV, $P < 0.05$) and a 1.4-mM increase in collected fluid HCO_3^- concentration ($P < 0.05$). Then, raising bafilomycin concentration to 10 nM significantly decreased net

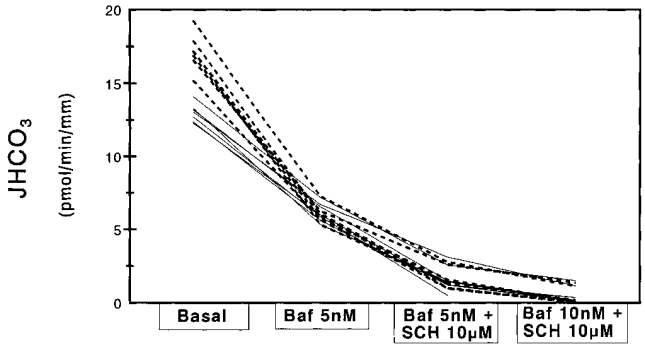

Figure 4. Effect of 5 nM bafilomycin A1 (*Baf 5nM*), 5 nM bafilomycin plus Sch 28080 (*Baf 5nM + SCH 10μM*), and 10 nM bafilomycin plus Sch 28080 (*Baf 10nM + SCH 10μM*) on net (*Basal*) HCO_3^- flux in OMCDs from control (*solid lines*, $n = 7$) and acid-treated (*dashed wide lines*, $n = 7$) rabbits. Each line represents an individual tubule experiment.

Table III. Mean Transport Data: Effect of Bafilomycin and Sch 28080

Parameter	Basal	Baf 5	Baf 5 + Sch	Baf 10 + Sch
Control OMCDs (n = 7)				
Tubule length (mm)	0.6±0.1			
Flow rate (nl/min)	1.9±0.1	1.9±0.1	1.8±0.1	1.7±0.1*‡
Perf. HCO_3^- (mmol/liter)	24.4±0.1	24.4±0.1	24.4±0.1	24.3±0.1
Coll. HCO_3^- (mmol/liter)	20.2±0.2	22.4±0.1*	23.8±0.1*‡	24.2±0.1*
J_{HCO_3} (pmol/min per mm)	13.0±0.2	6.2±0.3*	1.6±0.3*‡	0.6±0.3*‡
Acid OMCDs (n = 7)				
Tubule length (mm)	0.7±0.1			
Flow rate (nl/min)	1.9±0.1	1.8±0.1	1.7±0.1*	1.7±0.1*
Perf. HCO_3^- (mmol/liter)	24.3±0.1	24.3±0.1	24.3±0.1*‡	24.3±0.2*‡
Coll. HCO_3^- (mmol/liter)	18.2±0.3	22.1±0.1*	23.6±0.2*‡	24.1±0.2*‡
J_{HCO_3} (pmol/min per mm)	17.2±0.5	6.1±0.2*	1.7±0.3*‡	0.5±0.3*‡

OMCDs taken from control (*Control*) and acidotic (*Acid*) animals. Data are mean±SE (SE < 0.05 are rounded to 0.1). Perf. HCO_3^-, perfusion concentration of HCO_3^-; Coll. HCO_3^-, collected fluid concentration of HCO_3^-; J_{HCO_3}, net bicarbonate flux; Baf 5, 5 nM bafilomycin; Baf 5 + Sch, 5 nM bafilomycin plus 10 μM Sch28080; Baf 10 + Sch, 10 nM bafilomycin plus 10 μM Sch28080. *Significantly different from basal parameter; ‡significantly different from preceding period after basal.

HCO_3^- flux to nearly undetectable levels (0.6±0.3 pmol/min per mm, $P < 0.05$), and increased collected fluid HCO_3^- concentration to within 0.1 mM of the perfused concentration.

Similar results were obtained in seven segments from acidotic animals with a higher basal flux of 17.2±0.5 pmol/min per mm (Fig. 4, Table III) and a transepithelial voltage of 4.3±0.4 mV. Bafilomycin at 5 nM caused the flux to decrease by 11.1 pmol (65%) to 6.1±0.2 pmol/min per mm, voltage to decrease by 2 mV to 2.3±0.4 mV, and collected fluid HCO_3^- concentration to increase by 3.9 mM ($P < 0.01$ for all changes). The subsequent addition of Sch 28080 further decreased net flux by an additional 4.4 pmol to 1.7±0.3 pmol/min per mm ($P < 0.01$), decreased transepithelial voltage 0.2 mV (to 2.1±0.4 mV, $P < 0.05$), and increased collected fluid HCO_3^- concentration by 1.5 mM ($P < 0.05$). Raising bafilomycin concentration to 10 nM significantly decreased net HCO_3^- flux to 0.5±0.3 pmol/min per mm (not significantly different from zero), and increased collected fluid HCO_3^- concentration ($P < 0.05$) to within 0.2 mM of the perfused concentration.

These experiments allowed us to estimate the flux due to the H^+,K^+-ATPase from that which was sensitive to Sch 28080, and the difference was ascribed to that due to the H^+-ATPase (accounting within experimental error for 97% of the measured flux). Accordingly, we refer to the H,K flux and the H flux as the two main components comprising net HCO_3^- absorptive (or H^+ secretory) flux in the OMCD.

Paired comparisons of 2 H^+-ATPase and 2 H^+,K^+-ATPase inhibitors. To further validate these conclusions, we compared two specific inhibitors of H^+-ATPase (bafilomycin and concanamycin) and H^+,K^+-ATPase (Sch 28080 and luminal K^+ removal) in the same tubules. We made use of the observations that luminal K^+ removal (*a*) was reversible, and (*b*) in previous studies showed comparable inhibition to that observed with Sch 28080 (26, 31), and that (*c*) low concentrations of bafilomycin were also reversible (27, 31, 42).

In four OMCDs evaluated for H,K flux (Fig. 5, Table IV), the control net HCO_3^- flux was 13.3±0.1 pmol/min per mm. This flux was reversibly inhibited by 4.7 pmol (35%) to 8.6±0.1 pmol/min per mm by removing luminal K^+ ($P < 0.01$). A comparable inhibition of 4.7 pmol (35%) was then observed by applying 10 μM Sch 28080 to the luminal fluid, thus reducing the flux to 8.6±0.1 pmol/min per mm ($P < 0.01$). There was no change in transepithelial voltage, which averaged 3.7±0.2 mV with each of these maneuvers. Collected fluid HCO_3^- concentration was increased 1.7 mM by removal of luminal K^+ ($P < 0.05$), and was increased 1.5 mM by removal of Sch 28080 ($P < 0.05$) despite comparable perfusion flow rates in each period (Table IV). Thus, the two inhibitors of the P-type H^+,K^+-ATPase (luminal K^+ removal and Sch 28080) had quantitatively similar effects on net HCO_3^- transport, and no significant effect on transepithelial voltage.

Because there is some data showing that the H^+,K^+-ATPase may transport Na^+ in place of K^+ (41), we compared the effects of luminal Na^+ and K^+ removal versus luminal K^+ removal alone on net HCO_3^- transport. In three segments (Fig. 6, Table V) the basal flux was 12.5±0.7 pmol/min per mm. This flux was reversibly inhibited by 5.1 pmol to 7.4±0.4 pmol/min per mm (41%) by removing luminal K^+ and Na^+. After recovery, subsequent removal of luminal K^+ alone inhibited the flux

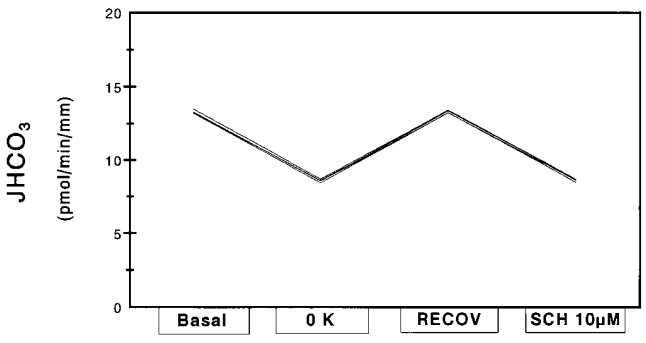

Figure 5. Effect of removing luminal K^+ (*0 K*) on net (*Basal*) HCO_3^- flux followed by Sch 28080 (*SCH 10 μM*) on recovery (*RECOV*) HCO_3^- flux. Each line represents an individual tubule experiment (n = 4). Basal and recovery fluxes were not significantly different from each other.

Table IV. Mean Transport Data: Effect of Luminal K^+ Removal vs. Sch 28080

Parameter	Basal	0 K	Recovery	Sch 28080
Control OMCDs (n = 4)				
Tubule length (min)	0.6±0.1			
Flow rate (nl/min)	1.8±0.1	1.8±0.1	1.8±0.1	1.7±0.1
Perf. HCO_3^- (mmol/liter)	24.5±0.1	24.4±0.1*	24.5±0.1	24.4±0.1
Coll. HCO_3^- (mmol/liter)	19.9±0.3	21.6±0.1*	19.9±0.5‡	21.4±0.3*‡
J_{HCO_3} (pmol/min per mm)	13.3±0.1	8.6±0.1*	13.3±0.1‡	8.6±0.1*‡

OMCDs taken from control (*Control*) animals. Data are mean±SE (SE < 0.05 are rounded to 0.1). Perf. HCO_3^-, perfusion concentration of HCO_3^-; Coll. HCO_3^-, collected fluid concentration of HCO_3^-; J_{HCO_3}, net bicarbonate flux; 0 K, luminal K^+ removal. Sch 28080, used at 10 μM; *Significantly different from basal parameter; ‡ significantly different from preceding period after basal.

Table V. Mean Transport Data: Effect of Luminal Na^+ and K^+ Removal vs. Luminal K^+ Removal

Parameter	Basal	0 Na,K	Recovery	0 K
Control OMCDs (n = 3)				
Tubule length (mm)	0.6±0.1			
Flow rate (nl/min)	1.9±0.1	1.8±0.1	1.9±0.1	1.6±0.1*
Perf. HCO_3^- (mmol/liter)	24.6±0.1	23.7±0.3	24.6±0.1	24.4±0.1*
Coll. HCO_3^- (mmol/liter)	20.6±0.1	21.2±0.2	20.5±0.4	21.7±0.2*‡
J_{HCO_3} (pmol/min per mm)	12.5±0.7	7.4±0.4*	12.2±0.8‡	7.3±0.4*‡

OMCDs taken from control (*Control*) animals. Data are mean±SE (SE < 0.05 are rounded to 0.1). Perf. HCO_3^-, perfusion concentration of HCO_3^-; Coll. HCO_3^-, collected fluid concentration of HCO_3^-; J_{HCO_3}, net bicarbonate flux; 0 Na,K, luminal Na^+ and K^+ removal; 0 K, luminal K^+ removal. *Significantly different from basal parameter; ‡significantly different from preceding period after basal.

by 4.9 pmol to 7.3±0.4 pmol/min per mm (40%). Collected fluid HCO_3^- concentration was increased 0.6 mM by removing luminal K^+ and Na^+ ($P < 0.05$), and was increased 1.2 mM by removing luminal K^+ ($P < 0.05$). The degree of H^+,K^+-ATPase inhibition was not significantly different whether or not Na^+ was present in the luminal fluid. These experiments allowed us to remove solely luminal K^+ to reversibly evaluate the H,K flux.

In four OMCDs evaluated for H flux (Fig. 7, Table VI) the control net HCO_3^- flux was 12.4±0.4 pmol/min per mm. This flux was reversibly inhibited by 7.0 pmol to 5.4±0.2 pmol/min per mm (57%) by adding 5 nM bafilomycin to the luminal fluid. Concomitantly, transepithelial voltage decreased by 1.4 mV (35%) from 4.0±0.1 to 2.6±0.2 mV ($P < 0.01$) with bafilomycin, while collected fluid HCO_3^- increased by 2.5 mM ($P < 0.05$), remaining 2.1 mM below the perfused concentration. A comparable inhibition of 6.9 pmol (56%) was then observed by applying 1 nM concanamycin to the luminal fluid, reducing HCO_3^- transport to 5.5±0.2 pmol/min per mm ($P < 0.01$); transepithelial voltage decreased by 1.1 mV (28%) from 3.9±0.1 to 2.8±0.2 mV ($P < 0.01$), while collected fluid HCO_3^- concentration increased by 2.1 mM ($P < 0.05$), remaining 2.1 mM below the perfused concentration. Elevating concanamycin concentration to 10 nM further inhibited HCO_3^- absorption by 0.8 pmol to 4.7±0.1 pmol/min per mm, and inhibited voltage by 0.4 mV to 2.4±0.2 mV ($P < 0.01$ for both). Collected fluid HCO_3^- concentration remained 1.8 mM smaller than the perfused concentration. The total concanamycin-sensitive flux (H flux) was 7.7 pmol/min per mm (62%) of the total net HCO_3^- flux. Thus, the two inhibitors of the vacuolar H^+-ATPase (bafilomycin and concanamycin) had quantitatively similar effects on net HCO_3^- transport. Moreover, we have accounted for nearly all of the net HCO_3^- flux measured in isolated perfused OMCD of the inner stripe: 62% was H flux and 35% was H,K flux. The remaining 3% was assumed to be H flux for the subsequent experiments that made use of luminal K^+ removal before and after a 3-h incubation.

Effect of in vivo acidosis on H flux and H,K flux. Using the removal of luminal K^+ to determine H,K flux (with the difference being H flux, as shown above to account for 97% of the total net HCO_3^- flux), we were able to estimate the contributions of H^+-ATPase and H^+,K^+-ATPase to net HCO_3^- absorption in OMCDs from 11 control and 11 acid-treated animals. There was no difference in H,K flux in OMCDs from control versus acid-treated animals (see Fig. 2) (control, 5.9±0.2 pmol/min per mm; acid, 5.8±0.2 pmol/min per mm; P = NS). Acid

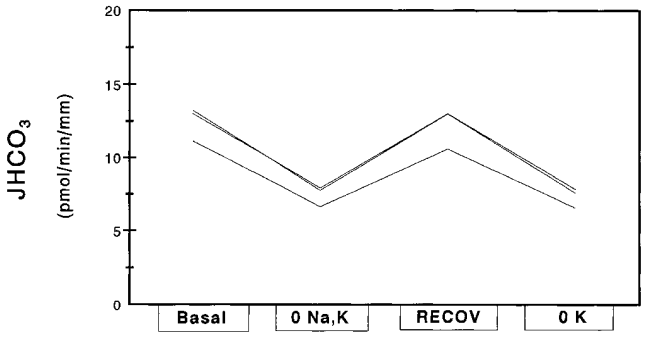

Figure 6. Effect of removing luminal Na^+ and K^+ (*0 Na,K*) on net (*Basal*) HCO_3^- flux followed by removing luminal K^+ (*0 K*) on recovery (*RECOV*) HCO_3^- flux. Each line represents an individual experiment (n = 3). Basal and recovery fluxes were not significantly different from each other.

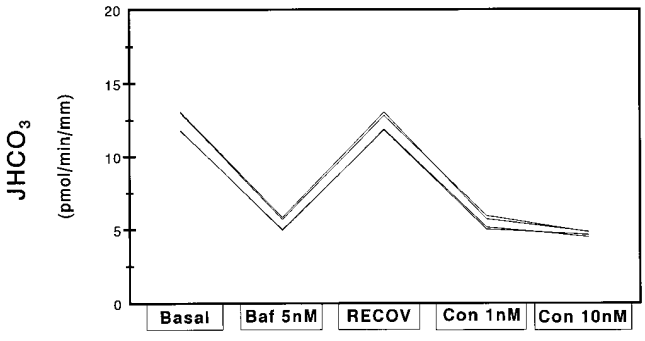

Figure 7. Effect of 5 nM bafilomycin (*Baf 5nM*) on net (*Basal*) HCO_3^- flux followed by 1 and 10 nM concanamycin (*Con 1nM, Con 10nM*) on recovery (*RECOV*) HCO_3^- flux. Each line represents an individual experiment (n = 4). Basal and recovery fluxes were not significantly different from each other.

Table VI. Mean Transport Data: Effect of Bafilomycin vs. Concanamycin

Parameter	Basal	Baf 5	Recovery	Con 1	Con 10
Control OMCDs ($n = 4$)					
Tubule length (mm)	0.6±0.1				
Flow rate (nl/mm)	1.7±0.1	1.7±0.1	1.9±0.1*‡	1.7±0.1	1.7±0.1
Perf. HCO_3^- (mmol/liter)	24.5±0.1	24.5±0.1	24.5±0.1	24.5±0.1‡	24.4±0.1
Coll. HCO_3^- (mmol/liter)	19.9±0.3	22.4±0.1*	20.3±0.2‡	22.4±0.1*‡	22.6±0.1*
J_{HCO_3} (pmol/min per mm)	12.4±0.4	5.4±0.2*	12.4±0.3‡	5.5±0.2*‡	4.7±0.1*‡

OMCDs taken from control animals. Data are mean±SE (SE < 0.05 are rounded to 0.1). Perf. HCO_3^-, perfusion concentration of HCO_3^-; Coll. HCO_3^-, collected fluid concentration of HCO_3^-; J_{HCO_3}, net bicarbonate flux; Baf 5, 5 nM bafilomycin; Con 1, 1 nM concanamycin; Con 10, 10 nM concanamycin. *Significantly different from basal parameter; ‡significantly different from preceding period after basal.

loading, however, appeared to induce significantly the H flux (Fig. 2) (control, 7.0±0.2 pmol/min per mm; acid, 11.3±0.2 pmol/min per mm; $P < 0.01$). The increment in H flux following acid treatment was 4.3 pmol. These data indicate that OMCDs from acid-treated rabbits secreted protons at a higher rate than OMCDs from control animals, and the observed adaptation occurred via changes in the vacuolar H^+-ATPase-dependent HCO_3^- flux.

Time course for acid incubation. To establish conditions for metabolic acidosis in vitro, we first performed three pilot studies to determine the minimum time required to stimulate H^+ secretion (HCO_3^- absorption) in isolated perfused OMCDs. After equilibration of one tubule, it was evident that a minimum of 3 h of incubation at pH 6.8 was necessary for clearcut stimulation (Table VII). In two other tubules, incubation for 1 h at pH 6.8 followed by 2 h at pH 7.4 achieved a comparable stimulation of H^+ secretion (Table VII). Shorter periods of incubation failed to stimulate reliably net HCO_3^- absorption.

Effect of in vitro acidosis on net HCO_3^- absorption. To better characterize the mechanism underlying this adaptation to in vivo metabolic acidosis, we incubated OMCDs from control animals for 1 h at pH 6.8 followed by 2 h at pH 7.4, as described above. In 5 OMCDs (Fig. 8, Table VIII) the baseline flux was 12.3±0.3 pmol/min per mm, and increased significantly to 16.2±0.3 after acid incubation ($P < 0.01$). The increment was 3.9 pmol (32%), comparable in magnitude to that observed in segments taken from acid-treated vs. control animals. Transepithelial voltage was increased 16% (0.7 mV) in parallel with the electrogenic H^+ pump (basal, 4.3±0.1 mV; acid-incubated, 5.0±0.1 mV; $P < 0.01$). Collected fluid HCO_3^- concentration was decreased by 1.5 mM from a mean of 19.9±0.3 mM to 18.4±0.4 mM after acid incubation ($P < 0.05$), despite comparable perfusion flow rates (Table VIII).

When this adaptation was analyzed for changes in specific fluxes, there was no change in H,K flux (solid and lower portion of stacked bars in Fig. 8; basal, 4.9±0.2 pmol/min per mm; acid-incubated, 4.7±0.2 pmol/min per mm; P = NS). There was, however, a 53% (4 pmol) increase in H flux (stippled portion of bars; basal, 7.5±0.2 pmol/min per mm; acid-incubated, 11.5±0.2 pmol/min per mm; $P < 0.01$). Again, the combination of inhibitors brought collected fluid HCO_3^- concentration to within 0.2 mM of the perfused concentration (Table VIII).

For time controls we incubated 4 OMCDs for 3 h at pH 7.4. There was no change in net flux, H,K, or H flux (Fig. 8), or transepithelial voltage (basal: 11.8±0.4 pmol/min per mm, 4.7±0.4 pmol/min per mm, 7.1±0.4 pmol/min per mm, and 3.9±0.4 mV, respectively; pH 7.4 incubated: 11.7±0.4 pmol/min per mm, 4.6±0.4 pmol/min per mm, 7.1±0.3 pmol/min per mm, and 3.9±0.3 mV, respectively; P = NS for each comparison). In addition, the collected fluid HCO_3^- concentrations before and after incubation at pH 7.4 were comparable in the presence or absence of luminal K^+ (Table IX).

Table VII. Time Course of Stimulation of H^+ Secretion In Three Outer Medullary Collecting Ducts

OMCD	Basal	pH	1h Pt	pH	2h Pt	pH	3h Pt
J_{HCO_3}1 (pmol/min per mm)	11.07	6.8	11.04	6.8	12.5	6.8	14.48
Vte (mV)	3.3		3.4		3.6		4.0
J_{HCO_3}2 (pmol/min per mm)	11.29	6.8	11.51	7.4	11.74	7.4	14.74
Vte (mV)	3.7		3.7		4.0		4.3
J_{HCO_3}3 (pmol/min per mm)	11.90	6.8	12.03	7.4	12.81	7.4	15.25
Vte (mV)	3.7		4.0		4.1		4.5

OMCD, outer medullary collecting duct; pH, pH of incubation for 1 h; Pt, point; J_{HCO_3}, net HCO_3^- absorptive flux; Vte, transepithelial voltage.

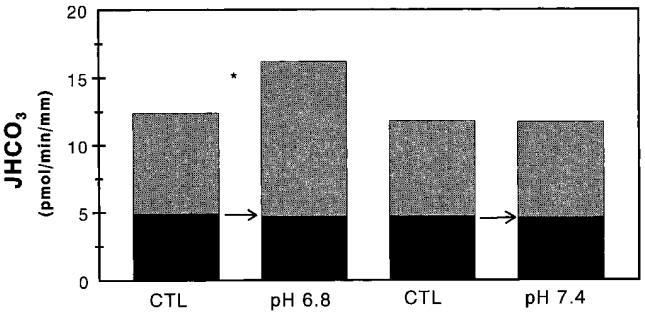

Figure 8. Effect of 3 h incubation on HCO_3^- transport, divided into components of H^+,K^+-ATPase- and H^+-ATPase-sensitive fluxes (H,K flux, *solid bar* on bottom, and H flux, *stippled bar* on top). Each pair of stacked bars indicates a basal condition from control animals (*CTL*) with an arrow pointing to the postincubation data. Incubation for 1 h at pH 6.8 followed by 2 h at pH 7.4 (*left side pair of stacked bars*) has been termed in vitro metabolic acidosis (pH 6.8); incubation for 3 h at pH 7.4 (*right side*) is a time control (*pH 7.4*). *Significantly different from basal condition, applying to the increase in H flux after incubation at pH 6.8.

Table VIII. Mean Transport Data for Acid-Incubated Tubules: Effect of Luminal K^+ Removal and Concanamycin

Parameter	Basal	0 K	Acid Inc.	0 K	0 K + Con 1	0 K + Con 10
Control OMCDs ($n = 5$)						
Tubule length (mm)	0.7±0.1					
Flow rate (nl/min)	1.9±0.1	1.8±0.1	1.9±0.1*‡	1.8±0.1	1.7±0.1*	1.7±0.1
Perf HCO_3^- (mmol/liter)	24.5±0.1	24.4±0.1*	24.6±0.1*‡	24.5±0.1‡	24.4±0.1*	24.3±0.1*
Coll. HCO_3^- (mmol/liter)	19.9±0.3	21.4±0.1*	18.4±0.4*‡	19.9±0.2‡	23.9±0.1*‡	24.1±0.1*‡
J_{HCO_3} (pmol/min per mm)	12.3±0.5	7.5±0.3*	16.2±0.8*‡	11.5±0.4‡	1.2±0.1*‡	0.4±0.1*‡
Acid OMCDs ($n = 6$)						
Tubule length (mm)	0.6±0.1					
Flow rate (nl/min)	1.9±0.1	1.8±0.1	1.8±0.1*‡	1.8±0.1	1.8±0.1	1.7±0.1*
Perf. HCO_3^- (mmol/liter)	24.5±0.1	24.4±0.1*	24.5±0.1*‡	24.4±0.1*‡	24.3±0.2*	24.3±0.1*
Coll. HCO_3^- (mmol/liter)	18.9±0.3	20.5±0.3*	17.2±0.5*‡	18.9±0.4‡	23.8±0.1*‡	24.1±0.2*‡
J_{HCO_3} (pmol/min per mm)	16.7±0.4	11.5±0.6*	21.3±0.5*‡	15.7±0.6*‡	1.4±0.3*‡	0.7±0.2*‡

OMCDs taken from control (*Control*) and acidotic (*Acid*) animals. Data are mean±SE (SE < 0.05 are rounded to 0.1). Perf. HCO_3^-, perfusion concentration of HCO_3^-; Coll. HCO_3^-, collected fluid concentration of HCO_3^-; J_{HCO_3}, net bicarbonate flux; 0 K, luminal K^+ removal; Acid Inc., after 3 h acid incubation; 0 K + Con 1, luminal K^+ removal plus 1 nM concanamycin; Con 10, 10 nM concanamycin. *Significantly different from basal parameter, ‡significantly different from preceding period after basal.

Effect of in vitro acidosis on net HCO_3^- absorption in OMCDs from acid-reated animals. To better understand the mechanism of adaptation of the OMCD in response to acidosis, we investigated whether tubules from in vivo acid-treated animals and tubules exposed to low pH in vitro could further regulate HCO_3^- transport. In six OMCDs from acid-treated animals (Fig. 9, Table VIII) the baseline flux was 16.7±0.3 pmol/min per mm, and increased significantly to 21.3±0.3 after acid incubation ($P < 0.01$). The increment was 4.6 pmol (28%), comparable in magnitude to that observed in segments from control animals incubated under similar conditions. Transepithelial voltage increased by 11% (0.6 mV) in parallel with the electrogenic H^+ pump (basal, 5.5±0.3 mV; acid-incubated, 6.1±0.4 mV; $P < 0.01$). Collected fluid HCO_3^- concentration decreased by 1.7 mM ($P < 0.05$) from a mean of 18.9±0.3 to 17.2±0.5 mM after acid incubation, despite comparable perfusion flow rates (Table VIII).

When this adaptation was analyzed for changes in specific fluxes, there was no change in H,K flux (solid portion of bars in Fig. 9; basal: 5.5±0.3 pmol/min per mm; acid-incubated: 5.6±0.3 pmol/min per mm; P = NS). There was, however, a 37% (4.2 pmol) increase in H flux (stippled part of bars; basal, 7.5±0.2 pmol/min per mm; acid-incubated, 11.5±0.2 pmol/min per mm; $P < 0.01$). This increment was comparable to what was observed in OMCDs taken from control animals and exposed to acid incubation, and thereby represents an additive effect of in vivo acidosis plus in vitro acidosis. The combination of inhibitors brought collected fluid HCO_3^- con-

Table IX. Mean Transport Data for pH 7.4-Incubated Tubules Effect of Luminal K^+ Removal and Concanamycin

Parameter	Basal	0 K	pH 7.4 Inc.	0 K	0 K + Con 1	0 K + Con 10
Control OMCDs ($n = 4$)						
Tubule length (mm)	0.7±0.1					
Flow rate (nl/min)	2.0±0.1	1.8±0.1	1.8±0.1*‡	1.8±0.1	1.7±0.1*	1.5±0.1*
Perf HCO_3^- (mmol/liter)	24.4±0.1	24.3±0.1*	24.4±0.1*‡	24.3±0.1*‡	24.3±0.1*	24.2±0.1*‡
Coll. HCO_3^- (mmol/liter)	20.5±0.1	21.7±0.2*	20.2±0.2‡	21.7±0.2*‡	23.9±0.1*‡	24.1±0.1*
J_{HCO_3} (pmol/min per mm)	11.8±0.6	7.1±0.4*	11.7±0.6‡	7.1±0.5*‡	1.0±0.1*‡	0.2±0.1*‡
Acid OMCDs ($n = 5$)						
Tubule length (mm)	0.7±0.1					
Flow rate (nl/min)	1.9±0.1	1.9±0.1	1.8±0.1	1.8±0.1*	1.7±0.1	1.6±0.1*
Perf HCO_3^- (mmol/liter)	24.5±0.1	24.4±0.1*	24.5±0.1*‡	24.4±0.1*‡	24.3±0.1*‡	24.3±0.1*
Coll. HCO_3^- (mmol/liter)	18.4±0.3	20.0±0.2*	18.6±0.3‡	20.2±0.3*‡	23.9±0.1*‡	24.2±0.1*‡
J_{HCO_3} (pmol/min per mm)	16.3±0.3	11.6±0.3*	15.2±0.3‡	10.4±0.5*‡	0.9±0.1*‡	0.2±0.1*‡

OMCDs taken from control (*Control*) and acidotic (*Acid*) animals. Data are mean±SE (SE < 0.05 are rounded to 0.1). Perf. HCO_3^-, perfusion concentration of HCO_3^-; Coll. HCO_3^-, collected fluid concentration of HCO_3^-; J_{HCO_3}, net bicarbonate flux; 0 K, luminal K^+ removal; pH 7.4 Inc., after 3 h incubation at pH 7.4; 0 K + Con 1, luminal K^+ removal plus 1 nM concanamycin; Con 10, 10 nM concanamycin. *Significantly different from basal parameter; ‡significantly different from preceding period after basal.

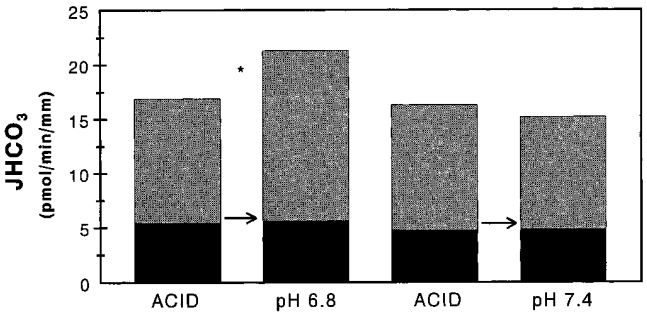

Figure 9. Effect of 3 h incubation on HCO_3^- transport, divided into components of H^+,K^+-ATPase- and H^+-ATPase-sensitive fluxes (H,K flux, *solid bar* on bottom and H flux, *stippled bar* on top). Each pair of stacked bars indicates a basal condition from acid-treated animals (*ACID*) with an arrow pointing to the post-incubation data. Incubation for 1 h at *pH 6.8* followed by 2 h at *pH 7.4* (*left side* pair of stacked bars) has been termed in vitro metabolic acidosis (*pH 6.8*); incubation for 3 h at pH 7.4 (*right side*) is a time control. *Significantly different from basal condition, applying to the increase in H flux after incubation at pH 6.8.

centration to within 0.2 mM of the perfused concentration (Table VIII).

For time controls, we incubated five OMCDs taken from acid-treated animals for 3 h at pH 7.4. After this incubation there were small changes in HCO_3^-, H,K, and H fluxes (Fig. 9), and transepithelial voltage that bordered on significance (basal: 16.3±0.3 pmol/min per mm, 4.7±0.3 pmol/min per mm, 11.6±0.3 pmol/min per mm, and 5.6±0.3 mV, respectively; pH 7.4-incubated: 15.2±0.4 pmol/min per mm, 4.8±0.3 pmol/min per mm, 10.4±0.4 pmol/min per mm, and 5.4±0.2 mV, respectively; $P = 0.06$, 0.05, 0.06, and 0.05, respectively). The collected fluid HCO_3^- concentrations were comparable before and after incubation at pH 7.4 in the presence or absence of luminal K^+ (Table IX).

Discussion

These studies are the first to show that the OMCD from the inner stripe responds to metabolic acidosis by increasing H^+ secretion, an adaptation that is appropriate for maintaining acid–base homeostasis of the animal. Previous studies have not shown functional regulation at the level of the OMCD in response to acidosis (8–11, 35), although other segments of the distal nephron, including the CCD (8, 9, 25, 31–33, 35, 43) and IMCD (4–6), have been shown to adapt to acidosis. Therefore, it is surprising that adaptation has not previously been demonstrated in this segment (7). Indeed, in a recent series of studies in the CCD, we found initially that a response to in vitro acidosis could not be demonstrated in α-intercalated cells, but were confined primarily to decreased HCO_3^- secretion by β-intercalated cells (10, 44). When we focused carefully on α-intercalated cell function in the CCD using specific inhibitors of the vacuolar H^+ pump and basolateral Cl^--HCO_3^- exchanger (31), however, we were able to show that increased H^+ secretion in response to in vitro acidosis occurred.

Using a monoclonal antibody directed against the 31-kD subunit protein of the vacuolar H^+-ATPase, Bastani et al. (24) showed rapid and striking changes in the immunocytochemical distribution of H^+-ATPase in the inner stripe of outer medulla from acidotic rats versus controls. Most of the cells showed a loss of vesicular cytoplasmic staining, with all of the label appearing on the apical membrane in a rim pattern within 1 d of acid treatment. Control rats showed few rim-labeled cells, with most of the antibody staining in a cytoplasmic vesicular pattern. Presumably the polarization of the H^+-ATPase would be an appropriate adaptive response that would mediate enhanced H^+ secretion in the OMCD. The findings of Bastani et al. agree with the morphologic studies of Madsen and Tisher (14) in the intercalated cells of the rat outer medulla. Using morphometric analysis and comparing to control rats, they showed a significant increase in surface density of the apical plasma membrane, along with a striking depletion of apical tubulovesicular structures in intercalated cells from kidneys of chronic acid-loaded rats. Thus, based on these careful immunocytochemical and electron microscopic studies, it is surprising that previous transport studies have failed to show adaptive increases in H^+ secretion (HCO_3^- absorption) in the OMCD.

Our investigation of the details of this regulation in the OMCD in response to metabolic acidosis indicate that it occurs via increased activity of the vacuolar H^+-ATPase, and not of the H^+,K^+-ATPase. This finding was demonstrated in two different ways: (*a*) in vivo acid treatment, and (*b*) in vitro acid incubation. We generated metabolic acidosis in rabbits using chronic 3 d NH_4Cl loading and restriction of chow, as previously described (28, 29). We compared animals of comparable weight and age, and always limited our perfused segments to the deep inner stripe of the outer medulla. In view of the marked cellular heterogeneity along the distal nephron (14, 15, 17, 20, 22), failure to obtain consistently segments from the same region of the outer medulla is likely to increase scatter among the transport data obtained from multiple animals. Moreover, in our study, basal net HCO_3^- flux in OMCDs from the inner stripe was significantly correlated with weight of the animal, such that the predicted flux from a 1.5 kg animal was 2.3 pmol less than that from a 2.5-kg rabbit (see Fig. 1; this is about half the total adaptation observed during in vivo metabolic acidosis).

To investigate the mechanisms of acidification in this segment, and to minimize the concerns regarding the specificity of any single pharmacologic agent, we used two different inhibitors of each of the known H^+-secreting ATPases. We used bafilomycin A_1 and concanamycin A to inhibit the vacuolar H^+-ATPase (27, 36–39), and Sch 28080 and luminal K^+ removal to inhibit the P-type H^+,K^+-ATPase (25–27, 37, 41, 45). Previous studies have indicated that bafilomycin or concanamycin in the nanomolar range had little inhibitory effect on F_1F_0 (F-type) or E_1E_2 (P-type) ATPases (36, 37, 46). Similarly, Sch 28080 in the micromolar range was found previously to inhibit collecting duct H^+,K^+-ATPase activity without affecting Na^+,K^+-ATPase or H^+-ATPase activity (47), or the Na^+-independent rate of intracellular pH recovery from an acid load in cultured OMCD cells (48). Luminal K^+ removal has no short-term toxicity, and inhibits HCO_3^- transport to an extent comparable to that of Sch 28080 (26). One cannot rule out, however, the possibility that our inhibitors, through other mechanisms, might have influenced HCO_3^- transport. The inhibition of HCO_3^- absorptive flux in the present studies was comparable for bafilomycin versus concanamycin, and for Sch 28080 versus luminal K^+ removal. The results allowed us to account for 97% of the net HCO_3^- absorption (H^+ secretion) rate. We consistently

found that 35% of the rate was due to the P-type H^+,K^+-ATPase (H,K flux), and 65% was because of the vacuolar H^+-ATPase (H flux).

These data differ somewhat from those of Wingo's laboratory (26, 27, 49), which show ~ 70% of HCO_3^- flux is sensitive to inhibition of H^+,K^+-ATPase, and only 30% to inhibition of the vacuolar H^+-ATPase. The results do agree in that the combination of inhibitors totally eliminates net HCO_3^- absorption (27), indicating that the vacuolar H^+-ATPase and the P-type H^+,K^+-ATPase are the two main proton pumps in the OMCD of the inner stripe. Perhaps different diets or slightly different perfused sections of the inner stripe OMCD yielded slightly different findings. In addition, the transepithelial voltages observed by us were somewhat lower than those observed previously by others (19, 26, 27). The changes observed, however, after stimulation of H^+ secretion in vitro or in vivo, or after inhibition of H^+ secretion by specific H^+-ATPase inhibitors, were in the directions expected for an electrogenic proton pump. Note that Armitage and Wingo did not see any reduction of positive transepithelial voltage by bafilomycin (27), a finding that differs from that observed in the present study and in a previous one in the HCO_3^--absorbing CCD (31). Furthermore, our data are more in line with those in perfused OMCDs published by Hays and Alpern which showed that *N*-ethylmaleimide (a less specific H^+-ATPase inhibitor), but not Sch 28080, inhibited the initial rate of Na^+-independent cell pH recovery from an intracellular acid load (50), and with those in cultured OMCD cells published by Manger and Koeppen (48) which showed that bafilomycin (a specific H^+-ATPase inhibitor) completely inhibited Na^+-independent cell pH recovery from an intracellular acid load.

Using the specific inhibitors and comparing OMCDs taken from acid-loaded and control rabbits, we found that in vivo acidosis caused a 4-pmol elevation in net HCO_3^- flux, entirely mediated by a 56% increase in vacuolar H^+-ATPase-mediated net HCO_3^- absorption (H flux). Acidosis in vivo did not have an effect on H^+,K^+-ATPase-mediated HCO_3^- absorption (H,K flux). These findings are also consistent with those of Fejes-Toth and Naray-Fejes-Toth (51), which showed up-regulation of H^+-ATPase 31-kD subunit mRNA expression in α-intercalated cells of acid-loaded compared to alkali-loaded rabbits, and of Garg and Narang (52), who showed increased *N*-ethylmaleimide-sensitive ATPase activity during acidosis. Despite the disclaimer in their abstract, Bastani et al. (24) showed slight elevations in 31 kD H^+-ATPase/β-actin mRNA ratios in 3 d acidotic versus control rat kidney medullas, which also could support our results. Our findings, however, do not agree with preliminary studies of Komatsu and Garg (53), which showed a 53% stimulation of ouabain-insensitive K-ATPase activity in the OMCD of the acidotic rat. Whether or not species or methodological differences could account for the up-regulation of this activity cannot at present be determined from their abstract. Indeed, our unpaired data show that the H,K flux from 11 OMCDs from control animals (5.9±0.2 pmol/min per mm) was not different from that of 11 OMCDs from acid-loaded animals (5.8±0.2 pmol/min per mm, P = NS); that is, chronic metabolic acidosis did not induce H^+,K^+-ATPase dependent H^+ secretion.

To further investigate the mechanisms of adaptation, we used a model of metabolic acidosis in vitro (31, 44) which previously was shown to induce CCDs to reverse polarity of net HCO_3^- flux from secretion to absorption. As shown in Table VII and Fig. 8, exposure to 1 h pH 6.8 followed by 2 h recovery at pH 7.4 was sufficient to induce consistent increases in net HCO_3^- absorption. When the contributions to the net HCO_3^- flux were determined in paired analyses, it was evident that the in vitro acid incubation exclusively stimulated H^+-ATPase-sensitive flux (H flux) by approximately 4 pmol (53%), and there was a concomitant increase in positive transepithelial voltage of 0.7 mV. No significant change was observed in H^+,K^+-ATPase-sensitive HCO_3^- flux (H,K flux). Time control experiments for 3 h at pH 7.4 did not affect HCO_3^- flux or transepithelial voltage, indicating that our OMCD preparation was stable for the duration of the experiment (7–8 h).

These findings indicate that adaptation to acidosis may occur within 3 h. The cellular mechanisms responsible for the large increase in H flux must be investigated further in a future study, but presumably directed protein and RNA synthesis could mediate these adaptive changes in OMCD function. Another possibility that explains the shifts in H^+-ATPase toward the apical membrane after acid loading (24), the increase in apical membrane surface and decrease in area of apical cytoplasmic vesicles (14), as well as the increase in H^+ secretion, would be activation of apical exocytosis and fusion of vesicles containing H^+ pumps with the apical membrane (54, 55). Such membrane recycling has previously been shown to occur in intercalated cells, and reptilian analogues in response to CO_2 (55–58). Some intercalated cells are also capable of high rates of apical endocytosis (32, 33, 54, 59), particularly when the stimulus to acidification has been removed (32, 54). These studies indicate that a mechanism of rather rapid adaptation would result from the exocytotic fusion with the apical membrane of vesicles containing H^+ pumps. The advantage of our in vitro acidosis model is that it allows direct testing of this hypothesis.

Our last group of experiments provided some additional information regarding the mechanisms underlying the adaptation to acidosis. We used tubules from acid-treated rabbits, and exposed them to acid incubation in vitro. We consistently observed, in addition to a higher basal H^+ secretory rate (16.7±0.4 pmol/min per mm), that acid incubation further stimulated H^+ secretion in an additive fashion (+4.6±0.3 pmol). The final (adapted to in vivo and in vitro acidosis) observed net HCO_3^- flux of 21.3±0.5 pmol was more than 70% higher than the basal rate of tubules taken from control animals, and the calculated H flux was more than twice that observed in control tubules. Using the above morphologic and immunocytochemical information, we believe that in vivo acidosis caused the synthesis of new H^+ pumps, many of which had been moved to the apical membrane by exocytosis to raise the rate of H^+ secretion in the OMCD. The additional stimulus of in vitro acidosis may induce apical exocytosis to fuse more H^+ pumps on the apical membrane, further raising the rate of H^+ secretion in the OMCD.

In summary, this is the first study to show physiologic adaptation of the OMCD of the inner stripe to chronic metabolic acidosis. The adaptation was comparable in tubules taken from rabbits with acidosis in vivo versus those taken from control animals and subjected to acid incubation in vitro. The in vivo and in vitro effects were additive, indicating the likelihood that exocytosis of proton pumps plus the synthesis of new proton pumps mediate the adaptations, as had been suggested from previous morphologic and immunocytochemical studies.

Acknowledgments

We are grateful for the technical assistance of Ms. J. Jenkins, and to Dr. M. Flessner for reading the manuscript.

Dr. Tsuruoka was supported by a postdoctoral fellowship award from the American Heart Association New York State Affiliate. Dr. Schwartz was supported by National Institutes of Health grant DK50603.

References

1. Akiba, T., V.K. Rocco, and D.G. Warnock. 1987. Parallel adaptation of the rabbit renal cortical sodium/proton antiporter and sodium/bicarbonate cotransporter in metabolic acidosis and alkalosis. *J. Clin. Invest.* 80:308–315.

2. Preisig, P.A., and R.J. Alpern. 1988. Chronic metabolic acidosis causes an adaptation in the apical membrane Na/H antiporter and basolateral membrane $Na(HCO_3)_3$ symporter in the rat proximal convoluted tubule. *J. Clin. Invest.* 82: 1445–1453.

3. McKinney, T.D., and M.B. Burg. 1977. Bicarbonate transport by rabbit cortical collecting tubules. *J. Clin. Invest.* 60:766–768.

4. Graber, M.L., H.H. Bengele, E. Mroz, C. Lechene, and E.A. Alexander. 1981. Acute metabolic acidosis augments collecting duct acidification rate in the rat. *Am. J. Physiol.* 241:F669–F676.

5. Bengele, H.H., J.H. Schwartz, E.R. McNamara, and E.A. Alexander. 1986. Chronic metabolic acidosis augments acidification along the inner medullary collecting duct. *Am. J. Physiol.* 250:F690–F694.

6. Wall, S.M., J.M. Sands, M.F. Flessner, H. Nonoguchi, K.R. Spring, and M.A. Knepper. 1990. Net acid transport by isolated perfused inner medullary collecting ducts. *Am. J. Physiol.* 258:F75–F84.

7. Schuster, V.L. 1993. Function and regulation of collecting duct intercalated cells. *Annu. Rev. Physiol.* 55:267–288.

8. Lombard, W.E., J.P. Kokko, and H.R. Jacobson. 1983. Bicarbonate transport in cortical and outer medullary collecting tubules. *Am. J. Physiol.* 244: F289–F296.

9. Atkins, J.L., and M.B. Burg. 1985. Bicarbonate transport by isolated perfused rat collecting ducts. *Am. J. Physiol.* 249:F485–F489.

10. Laski, M.E., and N.A. Kurtzman. 1990. Collecting tubule adaptation to respiratory acidosis induced in vivo. *Am. J. Physiol.* 258:F15–F20.

11. McKinney, T.D., and K.K. Davidson. 1987. Bicarbonate transport in collecting tubules from outer stripe of outer medulla of rabbit kidneys. *Am. J. Physiol.* 253:F816–F822.

12. Ishibashi, K., S. Sasaki, N. Yoshiyama, T. Shiigai, and J. Takeuchi. 1987. Generation of pH gradient across the rabbit collecting duct segments perfused in vitro. *Kidney Int.* 31:930–936.

13. McKinney, T.D., and K.K. Davidson. 1988. Effects of respiratory acidosis on HCO_3^- transport by rabbit collecting tubules. *Am. J. Physiol.* 255:F656–F665.

14. Madsen, K.M., and C.C. Tisher. 1984. Response of intercalated cells of rat outer medullary collecting duct to chronic metabolic acidosis. *Lab. Invest.* 51:268–276.

15. Verlander, J.W., K.M. Madsen, J.K. Cannon, and C.C. Tisher. 1994. Activation of acid-secreting intercalated cells in rabbit collecting duct with ammonium chloride loading. *Am. J. Physiol.* 266:F633–F645.

16. Alper, S.L., J. Natale, S. Gluck, H.F. Lodish, and D. Brown. 1989. Subtypes of intercalated cells in rat kidney collecting duct defined by antibodies against erythroid band 3 and renal vacuolar H^+-ATPase. *Proc. Natl. Acad. Sci. USA.* 86:5429–5433.

17. Schuster, V.L., G. Fejes-Toth, A. Naray-Fejes-Toth, and S. Gluck. 1991. Colocalization of H^+ ATPase and band 3 anion exchanger in rabbit collecting duct intercalated cells. *Am. J. Physiol.* 260:F506–F517.

18. Stone, D.K., D.W. Seldin, J.P. Kokko, and H.R. Jacobson. 1983. Anion dependence of rabbit medullary collecting duct acidification. *J. Clin. Invest.* 71: 1505–1508.

19. Stokes, J.B. 1982. Ion transport by the cortical and outer medullary collecting tubule. *Kidney Int.* 22:473–484.

20. Ridderstrale, Y., M. Kashgarian, B. Koeppen, G. Giebisch, D. Stetson, T. Ardito, and B. Stanton. 1988. Morphological heterogeneity of the rabbit collecting duct. *Kidney Int.* 34:655–670.

21. Weiner, I.D., C.S. Wingo, and L.L. Hamm. 1993. Regulation of intracellular pH in two cell populations of inner stripe of rabbit outer medullary collecting duct. *Am. J. Physiol.* 265:F406–F415.

22. Madsen, K.M., J.W. Verlander, J. Kim, and C.C. Tisher. 1991. Morphological adaptation of the collecting duct to acid-base disturbances. *Kidney Int.* 40 (Suppl. 33):57–63.

23. Brown, D., S. Hirsch, and S. Gluck. 1988. Localization of a proton-pumping ATPase in rat kidney. *J. Clin. Invest.* 82:2114–2126.

24. Bastani, B., H. Purcell, P. Hemken, D. Trigg, and S. Gluck. 1991. Expression and distribution of renal vacuolar proton-translocating adenosine triphosphatase in response to chronic acid and alkali loads in the rat. *J. Clin. Invest.* 88:126–136.

25. Gifford, J.D., L. Rome, and J.H. Galla. 1992. H^+-K^+-ATPase activity in rat collecting duct segments. *Am. J. Physiol.* 262:F692–F695.

26. Armitage, F.E., and C.S. Wingo. 1995. Luminal acidification in K-replete $OMCD_i$: inhibition of bicarbonate absorption by K removal and luminal Ba. *Am. J. Physiol.* 269:F116–F124.

27. Armitage, F.E., and C.S. Wingo. 1994. Luminal acidification in K-replete $OMCD_i$: contributions of H-K-ATPase and bafilomycin-A_1-sensitive H-ATPase. *Am. J. Physiol.* 267:F450–F458.

28. Brion, L.P., B.J. Zavilowitz, C. Suarez, and G.J. Schwartz. 1994. Metabolic acidosis stimulates carbonic anhydrase activity in rabbit proximal tubule and medullary collecting duct. *Am. J. Physiol.* 266:F185–F195.

29. Schwartz, G.J., C.A. Winkler, B.J. Zavilowitz, and T. Bargiello. 1993. Carbonic anhydrase II mRNA is induced in the rabbit kidney cortex during chronic metabolic acidosis. *Am. J. Physiol.* 265:F764–F772.

30. Burg, M., and N. Green. 1977. Bicarbonate transport by isolated perfused rabbit proximal tubules. *Am. J. Physiol.* 233:F307–F314.

31. Tsuruoka, S., and G.J. Schwartz. 1996. Adaptation of rabbit cortical collecting duct HCO_3^- transport to metabolic acidosis in vitro. *J. Clin. Invest.* 97: 1076–1084.

32. Satlin, L.M., and G.J. Schwartz. 1989. Cellular remodeling of HCO_3^--secreting cells in rabbit renal collecting duct in response to an acidic environment. *J. Cell Biol.* 109:1279–1288.

33. Schwartz, G.J., J. Barasch, and Q. Al-Awqati. 1985. Plasticity of functional epithelial polarity. *Nature (Lond.).* 318:368–371.

34. Schwartz, G.J., A.M. Weinstein, R.E. Steele, J.L. Stephenson, and M.B. Burg. 1981. Carbon dioxide permeability of rabbit proximal convoluted tubules. *Am. J. Physiol.* 240:F231–F244.

35. Hamm, L.L., K.S. Hering-Smith, and V.M. Vehaskari. 1989. Control of bicarbonate transport in collecting tubules from normal and remnant kidneys. *Am. J. Physiol.* 256:F680–F687.

36. Drose, S., K.U. Bindseil, E.J. Bowman, A. Siebers, A. Zeeck, and K. Altendorf. 1993. Inhibitory effect of modified bafilomycins and concanamycins on P- and V-type adenosinetriphosphatases. *Biochemistry.* 32:3902–3906.

37. Mattsson, J.P., K. Vaananen, B. Wallmark, and P. Lorentzon. 1991. Omeprazole and bafilomycin, two proton pump inhibitors: differentiation of their effects on gastric, kidney and bone H^+-translocating ATPases. *Biochim. Biophys. Acta.* 1065:261–268.

38. Werner, G., and H. Hagenmaier. 1984. Metabolic products of microorganisms. 224. Bafilomycins, a new group of macrolide antibiotics. Production, isolation, chemical structure, and biological activity. *J. Antibiot. (Tokyo).* 37: 110–117.

39. Kinashi, H., K. Someno, and K. Sakaguchi. 1984. Isolation and characterization of concanamycins A, B, and C. *J. Antibiot.* 37:1333–1343.

40. Zhou, X., and C.S. Wingo. 1994. Stimulation of total CO_2 flux by 10% CO_2 in rabbit CCD: role of an apical Sch-28080- and Ba-sensitive mechanism. *Am. J. Physiol.* 267:F114–F120.

41. Zhou, X., and C.S. Wingo. 1992. Mechanisms of rubidium permeation by rabbit cortical collecting duct during potassium restriction. *Am. J. Physiol.* 263:F1134–F1141.

42. Yoshimori, T., A. Yamamoto, Y. Moriyama, M. Futai, and Y. Tashiro. 1991. Bafilomycin A_1, a specific inhibitor of vacuolar-type H^+-ATPase, inhibits acidification and protein degradation in lysosomes of cultured cells. *J. Biol. Chem.* 266:17707–17712.

43. McKinney, T.D., and M.B. Burg. 1978. Bicarbonate secretion by rabbit cortical collecting tubules in vitro. *J. Clin. Invest.* 61:1421–1427.

44. Yasoshima, K., L.M. Satlin, and G.J. Schwartz. 1992. Adaptation of rabbit cortical collecting duct to in vitro acid incubation. *Am. J. Physiol.* 263:F749–F756.

45. Wallmark, B., C. Briving, J. Fryklund, K. Munson, R. Jackson, J. Mendlein, E. Rabon, and G. Sachs. 1987. Inhibition of gastric H^+,K^+-ATPase and acid secretion by SCH 28080, a substituted pyridyl(1,2a)imidazole. *J. Biol. Chem.* 262:2077–2084.

46. Bowman, E.J., A. Siebers, and K. Altendorf. 1988. Bafilomycins: A class of inhibitors of membrane ATPases from microorganisms, animal cells, and plant cells. *Proc. Natl. Acad. Sci. USA.* 85:7972–7976.

47. Cheval, L., C. Barlet-Bas, C. Khadouri, E. Feraille, S. Marsy, and A. Doucet. 1991. K^+-ATPase-mediated Rb^+ transport in rat collecting tubule: modulation during K^+ deprivation. *Am. J. Physiol.* 260:F800–F805.

48. Manger, T.M., and B.M. Koeppen. 1992. Characterization of acid–base transporters in cultured outer medullary collecting duct cells. *Am. J. Physiol.* 263:F996–F1003.

49. Wingo, C.S., and A.J. Smolka. 1995. Function and structure of H-K-ATPase in the kidney. *Am. J. Physiol.* 269:F1–F16.

50. Hays, S.R., and R.J. Alpern. 1990. Apical and basolateral membrane H^+ extrusion mechanisms in inner stripe of rabbit outer medullary collecting duct. *Am. J. Physiol.* 259:F628–F635.

51. Fejes-Toth, G., and A. Naray-Fejes-Toth. 1995. Effect of acid/base balance on H-ATPase 31 kD subunit mRNA levels in collecting duct cells. *Kidney Int.* 48:1420–1426.

52. Garg, L.C., and N. Narang. 1985. Stimulation of an N-ethylmaleimide-sensitive ATPase in the collecting duct segments of the rat nephron by metabolic acidosis. *Can. J. Physiol. Pharmacol.* 63:1291–1296.

53. Komatsu, Y., and L.C. Garg. 1991. Stimulation of ouabain-insensitive K-ATPase in the rat medullary collecting duct by potassium depletion and metabolic acidosis. *FASEB J.* 5:752. (Abstr.)

54. Schwartz, G.J., and Q. Al-Awqati. 1986. Regulation of transepithelial H^+ transport by exocytosis and endocytosis. *Annu. Rev. Physiol.* 48:153–161.

55. Schwartz, G.J., and Q. Al-Awqati. 1985. Carbon dioxide causes exocytosis of vesicles containing H^+ pumps in isolated perfused proximal and collecting tubules. *J. Clin. Invest.* 75:1638–1644.

56. Gluck, S., C. Cannon, and Q. Al-Awqati. 1982. Exocytosis regulates urinary acidification in turtle bladder by rapid insertion of H^+ pumps into the luminal membrane. *Proc. Natl. Acad. Sci. USA.* 79:4327–4331.

57. Stetson, D.L., and P.R. Steinmetz. 1983. Role of membrane fusion in CO_2 stimulation of proton secretion by turtle bladder. *Am. J. Physiol.* 245: C113–C120.

58. Stetson, D.L., and P.R. Steinmetz. 1986. Correlation between apical intramembrane particles and H^+ secretion rates during CO_2 stimulation in turtle bladder. *Pflugers Arch. Eur. J. Physiol.* 407:80s–84s.

59. Brown, D., P. Weyer, and L. Orci. 1987. Nonclathrin-coated vesicles are involved in endocytosis in kidney collecting duct intercalated cells. *Anat. Rec.* 218:237–242.